Constrained Control Scheme for the Manipulation of Heavy Pre-fabricated Elements with Lightweight Robotic Arm

M. Ambrosino[1], F. Boucher [2], P. Mengeot [2], and E. Garone[1]

[1]Service d'Automatique et d'Analyse des Systèmes, Université Libre de Bruxelles, Brussels, Belgium.
[2] NV BESIX SA, Brussels, Belgium.

Michele.Ambrosino@ulb.ac.be, fabian.boucher@besix.com, pierre.mengeot@besix.com, egarone@ulb.ac.be

Abstract -

Building activities involving heavy suspended elements are one of the construction activities with the highest level of danger. Typically, during these activities, one or two masons work in conjunction with a machine such as a crane or a lifting machine. Several robotics solutions have been proposed to replace the masons during these hazard operations. In this work, we propose to use a lightweight robotic arm to handle and place a heavy suspended object ensuring a high level of precision during the planned operations. To control the resulting robotic system, we propose a constrained control scheme based on Explicit Reference Governor (ERG) theory, an add-on unit that modifies the applied reference in such a way that the trajectory of the system always fulfills the constraints of the system. The simulation results show the efficiency of our approach by testing it against other solutions proposed so far.

Keywords -

Robotics; Cooperative Robotic Systems; Building Activity; Robots for Construction; Constrained Control Scheme.

1 Introduction

Various construction activities are based on the handling and positioning of placement of prefabricated heavy elements, such as renovation of facades [1], or construction of walls [2]. These types of activities are carried out through the use of machines, such as cranes or lifting mechanisms, in which the object to be positioned is suspended through a cable. Then, the machine moves the object near its final position and a human being (e.g. a bricklayer), manually finishes the operation by guiding the suspended object for the last few centimeters. The presence of the bricklayer is necessary to ensure a high level of precision in the operations. However, these operations involve heavy suspended objects, which represent possible causes of accidents for the bricklayer (sometimes fatal) [3].

Several approaches have been proposed so far in the literature with the aim of using a robotic solution for this type of construction activity [4, 5]. For a complete overview of the drawbacks and the benefits of the proposed robotic solutions, please refer to [6].

Among the various solutions proposed so far, in this work we focus on the one discussed in [6, 7] in order to improve the preliminary proposed control strategies. The authors show how the cooperation between a crane and a industrial robotic arm is able to perform the positioning of heavy blocks in order to guarantee a high level of precision during masonry activities. The control laws proposed in these two researches are based on an *'ad-hoc'* trajectory for the positioning operations, and as highlighted by the authors themselves these control schemes should be reinforced with a governing unit that is capable of managing the constraints that are present in this type of operations. In particular, the main constraints that must to be considered concern the torque required to the actuators of the robotic arm used during operations. In fact, the robot having to handle a payload much heavier than the maximum permissible payload could find itself in an overload situation which would affect the robot itself.

In this paper we propose the design of a lightweight constrained control scheme for a robotic arm that unlike those proposed so far in the literature: *i*) it does not require any offline pre-evaluation of a feasible trajectory; *ii*) it does not solve any online optimization problems. Moreover, the proposed control scheme always fulfills the constraints of the system.

A general purpose control solution that is able to handle constraints in real-time is Model Predictive Control (MPC) [8]. MPC provides an optimal control strategy through the solution of an optimization problem at each sampling time. However, this kind of control schemes have a high computational cost with respect to simpler control schemes, especially when applied to nonlinear systems, therefore, in practice, its application is still limited [9]. A promising alternative to MPC is to consider a first inner controller to stabilize the system, and then, 'augment' the system with constraint-handling capabilities. This idea is the core of the Reference Governor (RG) schemes [10]. The RG is an add-on unit that filters the desired reference in such a way that the trajectory of the system always fulfills the

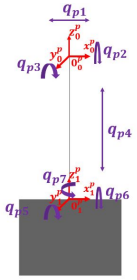

Figure 1. Suspended element configuration.

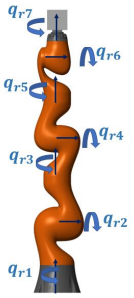

Figure 2. Robotic arm configuration.

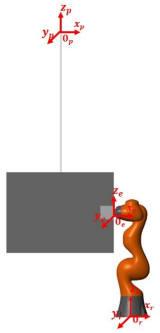

Figure 3. Frame configuration

constraints. However, as the MPC scheme, RGs rely on on-line optimization as well. To overcome this problem, in the past few years, a novel constrained control scheme that does not require on-line optimization was proposed, called the Explicit Reference Governor (ERG) [11, 12].

The aim of this paper is to implement a trajectory-based ERG for the handling activty of a heavy suspended elements with a lightweigth robotic arm. In the first part of this paper, a mathematical model of system under consideration will be derived. Next, the constrained control scheme used in this work is analyzed. At the end of this work the performances of the proposed control scheme are shown through simulations and compared to those proposed in the previous works in the literature.

2 Modeling

This section provides the general dynamic model of the system under consideration by systematically combing two types of model: a *suspended object*, and a *robotic arm*. The dynamic model of the two parts will be discussed separately. Then, the dynamic model of the entire system will be derived. More detailes about this kind of modeling can be found in [7].

2.1 Dynamic Model

The dynamic of the suspended element can be treated as that a of 7-DoF pendulum, see Fig.1. In particular, the configuration of the suspended object can be described by seven variables, $q_p \in \mathbb{R}^7$, where $q_p = \left[q_{p1}, q_{p2}, q_{p3}, q_{p4}, q_{p5}, q_{p6}, q_{p7}\right]^T$. Where q_{p1} is the displacement along the x-direction, q_{p4} is the length of the rope, q_{p2} and q_{p3} are the radial sway and the tangential pendulation respectively, and q_{p5}, q_{p6}, q_{p7} are the orientations of the block *w.r.t* the cable. It is worth noting that this kind of mechanical system is an underactuated system, having fewer independent actuators than system degrees of freedom (DoFs). In our work we consider the possibility of moving the object along the x axis and the z axis based on the fact that in real scenarios machines such as cranes can perform these two movements.

The robotic arm used in this paper is a 7-DoF robotic, and more precisely a KUKA IIWA14 R820 [13]. The robot configuration is described by the joint variables vector $q_r \in \mathbb{R}^7$, with $q_r = \left[q_{r1}, q_{r2}, q_{r3}, q_{r4}, q_{r5}, q_{r6}, q_{r7}\right]^T$, see Fig.2.

As shown in [6], the dynamic model of the whole system can be obtained introducing a set of closed-chain constraints that come when the robot has already grabbed the suspended object (see Fig.3). Therefore, the dynamic model of the constrained mechanical system can be compactly rewritten considering as state vector for the entire system the vector $q \in \mathbb{R}^{14}$, $q = \left[q_r, q_p\right]^T$, and using the equations:

$$B(q)\ddot{q}+C(q,\dot{q})\dot{q}+F\dot{q}+G(q) = u+A(q)^T\lambda-J(q)^T h_e \quad (1)$$

$$\text{s.t.} \qquad A(q)\dot{q} = 0, \quad (2)$$

where $A(q) \in \mathbb{R}^{6\times14}$, is the so-called *Jacobian* of the constraints, the matrices $B(q) \in \mathbb{R}^{14\times14}$, $C(q,\dot{q}) \in \mathbb{R}^{14\times14}$, $F(q) \in \mathbb{R}^{14\times14}$, and $G(q) \in \mathbb{R}^{14}$ represent the inertia, centripetal-Coriolis, friction matrix, and gravity term, respectively. Moreover, $\lambda \in \mathbb{R}^6$ is the vector of the *Lagrange*

multipliers, $h_e \in \mathbb{R}^6$ represents the vector of the forces generated by contact with the environment, $J(q) \in \mathbb{R}^{6\times14}$ is the manipulator geometric Jacobian [14], and $u \in \mathbb{R}^{14}$ is the vector of the control input of the system. As we highlighted before, the suspended object is modelled as an underactuated system, therefore the control input u is

$$u = [\tau_r, \tau_x, 0, 0, \tau_l, 0, 0, 0]^T, \tag{3}$$

where $\tau_r \in \mathbb{R}^7$ is the vector of the robot control input, τ_x is the object control input for the displacement along the x axis, and τ_l is the object control input for the displacement along the z axis. According to [6], the model (1) can be rewritten eliminating the Lagrangian multipliers as follows:

$$B(q)\ddot{q} = \left(I - A^T(q)A^{\star T}(q)\right)\left(u - J(q)^T h_e - m(q,\dot{q})\right) - B(q)A^{\star}(q)\dot{A}(q)\dot{q}, \tag{4}$$

where, $m(q,\dot{q}) = C(q,\dot{q})\dot{q} + F\dot{q} + G(q)$, and $A^{\star}(q)$ is the inertia-weighted pseudo-inverse of the constraint Jacobian A defined as

$$A^{\star}(q) = B^{-1}(q)A^T(q)(A(q)B^{-1}(q)A^T(q))^{-1}. \tag{5}$$

.

2.2 Control objective

The main goal of this paper is to propose a constrained control scheme for the system (4). This scheme must allow the system to follow a piece-wise constant reference $r(t) \in \mathbb{R}^9$ while ensuring that

i. for any piece-wise continuous reference $r(t)$, the control law guarantees constraint satisfaction of the state constraints;

ii. safe cooperation between the two sub-units is ensured, *i.e.* the robot will never be overloaded and the robot actuators torque limits are never violated;

iii. if the reference r is constant and steady-state admissible, the closed-loop system satisfies $\lim_{t\to\infty} q(t) = r(t)$.

In particular, in the development of our control law, we consider the following constraints:

- joint range constraints:

$$\begin{cases} q_{min,r,i} \le q_{r,i} \le q_{max,r,i} \\ q_{min,x} \le q_x \le q_{max,x} \\ q_{min,l} \le q_l \le q_{max,l} \end{cases}. \tag{6}$$

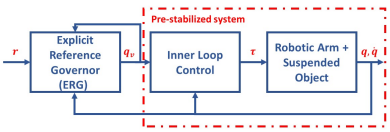

Figure 4. Control Scheme

for some lower and upper joint range limits $q_{min,r,i}$, $q_{max,r,i} \in \mathbb{R}$, $i = 1,\dots,7$ for the robotic arm, and $q_{min,x}$, $q_{max,x}$ and $q_{min,l}$, $q_{max,l}$ for the actuated joint of the suspended object.

- Maximum joint velocity constraints:

$$\begin{cases} \dot{q}_{min,r,i} \le \dot{q}_{r,i} \le \dot{q}_{max,r,i} \\ \dot{q}_{min,x} \le \dot{q}_x \le \dot{q}_{max,x} \\ \dot{q}_{min,l} \le \dot{q}_l \le \dot{q}_{max,l} \end{cases} \tag{7}$$

for some lower and upper joint velocity limits $\dot{q}_{min,r,i}$, $\dot{q}_{max,r,i} \in \mathbb{R}$, $i = 1,\dots,7$ for the robotic arm, and $\dot{q}_{min,x}$, $\dot{q}_{max,x}$ and $\dot{q}_{min,l}$, $\dot{q}_{max,l}$ for the actuated joint of the suspended object.

- Actuator saturation on the input:

$$\begin{cases} \tau_{min,r,i} \le \tau_{r,i} \le \tau_{max,r,i} \\ \tau_{min,x} \le \tau_x \le \tau_{max,x} \\ \tau_{min,l} \le \tau_l \le \tau_{max,l}, \end{cases} \tag{8}$$

for some lower and upper actuator limits $\tau_{min,r,i}$, $\tau_{max,r,i} \in \mathbb{R}$, $i = 1,\dots,7$ for the robotic arm, and $\tau_{min,x}$, $\tau_{max,x}$ and $\tau_{min,l}$, $\tau_{max,l}$ for the actuated joint of the suspended object.

3 Control Scheme

In this section, we describe the constraint control scheme used in our work. This scheme decouples the stabilization of the system and the satisfaction of the constraints: an *internal controller* fulfills the former task, whereas a *governing unit* modifies the reference fed to the system in such a way that constraints are fulfilled at all times. An illustration of this control architecture can be found in Fig. 4.

3.1 Internal Control Layer

As previously mentioned, the goal of the inner control loop is to stabilize the system without taking into account system constraints. This task can be performed

using a common control scheme based on a Proportional-Derivative (PD) action with gravity compensation. In particular,

- for the robotic arm:

$$\tau_r = K_{Pr}\tilde{q}_r - K_{D_r}\dot{q}_r + g_r(q_r), \tag{9}$$

- for the displacement along the x-axes:

$$\tau_x = K_{Px}\tilde{q}_x - K_{D_x}\dot{q}_x, \tag{10}$$

- to stabilize the length of the cable:

$$\tau_l = K_{Pl}\tilde{q}_l - K_{D_l}\dot{q}_l + g_l(q_p), \tag{11}$$

where $\tilde{q}_r = q_{vr} - q_r$, $\tilde{q}_x = q_{vx} - q_{p1}$, and $\tilde{q}_l = q_{vl} - q_{p4}$, with $q_v = [q_{vr}, q_{vx}, q_{vl}]^T \in \mathbb{R}^9$ being the vector of the applied reference associated to the commanded reference r. $K_{Pr} \in \mathbb{R}^{7\times7}$ and $K_{Dr} \in \mathbb{R}^{7\times7}$ are positive definite diagonal matrices, instead K_{Px}, K_{Dx}, K_{Pl}, and K_{Dl} are positive scalar gains. Instead, $g_r(q_r) \in \mathbb{R}^7$, and $g_l(q_p)$ represent the gravity compensation relating to the robotic arm and the cable length. It is possible to prove that the control laws (9)-(11) is able to pre-stabilize the system (4).

Lemma 1. Consider the system (4), the controller (9)-(11) makes every equilibrium configuration $q = [q_{vr}, q_{vx}, 0, 0, q_{vl}, 0, 0, 0]$, $\dot{q} = 0 \in R^{14}$ Globally Asymptotically Stable (GAS).

Proof. Please refer to [7].

3.2 Governing Unit: Trajectory-Based ERG

While the controller (9)-(10) ensure the asymptotically stability of the system, it is unable to manage the constraints (6)-(8). Therefore, in this paper we propose to augment the first inner control loop with a Governing Unit to be able to deal with the system constraints. In particular, the proposed governing unit belongs to the theory of the Explicit Reference Governor (ERG) [11]. In particular, rather than pre-computing a suitable trajectory $q_v(t)$, the ERG achieves these objectives by continuously manipulating the derivative of the applied reference as the product of two terms: the Navigation Field (NF) $\rho(q_v, r)$, and the Dynamic Safety Margin (DSM) $\Delta(q, \dot{q}, q_v)$. In particular, $\rho(q_v, r)$ is a vector field that generates the desired steady-state admissible path, and $\Delta(q, \dot{q}, q_v)$ is a scalar that quantifies the distance between the predicted transient dynamics of the pre-stabilized system and the constraint boundaries if the current $q_v(t)$ were to remain constant. More formally,

$$\dot{q}_v = \rho(q_v, r)\Delta(q, \dot{q}, q_v). \tag{12}$$

Since the set of admissible references is convex, the NF can be designed using an attraction and repulsion field [15],

$$\rho(q_v, r) = \rho^{\text{att}} + \rho^{\text{rep}}, \tag{13}$$

where the attraction field is

$$\rho^{\text{att}}(q_v, r) = \frac{r - q_v}{max(\|r - q_v\|, \eta)}, \tag{14}$$

and where $\eta > 0$ is a smoothing parameter ensuring ρ^{att} is a class C^1 function.

The repulsion field for the problem at hand can be expressed as the sum of two repulsion field, one for the position constraints and the second one for torque constraints, *i.e.*

$$\rho^{\text{rep}} = \rho^{\text{rep}}_{pos} + \rho^{\text{rep}}_{\tau}, \tag{15}$$

where

$$\rho^{\text{rep}}_{pos} = \left[\rho^{\text{rep}}_{1,pos}, ..., \rho^{\text{rep}}_{9,pos}\right]^T, \tag{16}$$

with

$$\begin{aligned}\rho^{\text{rep}}_{i,pos} = &\max\left(\frac{\zeta - |q_{v,i} - q_{min,i}|}{\zeta - \delta}, 0\right)\\ &-\max\left(\frac{\zeta - |q_{v,i} - q_{max,i}|}{\zeta - \delta}, 0\right),\end{aligned} \tag{17}$$

and

$$\rho^{\text{rep}}_{\tau} = \left[\rho^{\text{rep}}_{1,\tau}, ..., \rho^{\text{rep}}_{9,\tau}\right]^T, \tag{18}$$

with

$$\begin{aligned}\rho^{\text{rep}}_{i,\tau} = &\max\left(\frac{\zeta - |\tau_i - \tau_{min,i}|}{\zeta - \delta}, 0\right)\\ &-\max\left(\frac{\zeta - |\tau_i - \tau_{max,i}|}{\zeta - \delta}, 0\right),\end{aligned} \tag{19}$$

where $\delta > 0$ is the static safety margin of all the joint angles and $\zeta > \delta$ is the influence margin.

Among the different design tools for generating a suitable Dynamic Safety Margin (DSM), in this work we propose to use the trajectory based approach. The idea behind the trajectory-based ERG is to compute the trajectories of the pre-stabilized system $\hat{q}(t|q, \dot{q}, q_v) = \hat{q}_{t'=t}$, under the assumption that the current applied reference $q_v(t)$ is kept constant. The DSM is then characterized as the minimum distance of the trajectory to each of the constraints. The

trajectory can be obtained by simulating the forward dynamics of the system (4). We first initialize at the current time t the states that will be predicted, $\hat{q}$ and $\dot{q}$,

$$\begin{cases} \hat{\dot{q}}_{t'=t} = \dot{q}(t), \\ \hat{q}_{t'=t} = q(t), \end{cases} \tag{20}$$

Then we simulate the system dynamics using numerical integration as follows

$$\begin{cases} \hat{\tau}_{r,t'+dt} = K_{Pr}(q_{vr} - \hat{q}_{r,t'}) - K_{Dr}\hat{\dot{q}}_{r,t'} + g_r(\hat{q}_{r,t'}) \\ \hat{\tau}_{x,t'+dt} = K_{Px}(q_{vx} - \hat{q}_{x,t'}) - K_{Dx}\hat{\dot{q}}_{x,t'} \\ \hat{\tau}_{l,t'+dt} = K_{Pl}(q_{vl} - \hat{q}_{l,t'}) - K_{Dl}\hat{\dot{q}}_{l,t'} + g_r(\hat{q}_{l,t'}) \\ \ddot{q}_{t'+dt} = B(\hat{q}'_t)^{-1}\left(I - A^T(\hat{q}'_t)A^{\star T}(\hat{q}'_t)\right) \\ \left(\hat{u} - J(\hat{q}'_t)^T h_e - m(\hat{q}'_t, \hat{\dot{q}}'_t)\right) - B(\hat{q}'_t)A^{\star}(\hat{q}'_t)\dot{A}(\hat{q}'_t)\hat{\dot{q}}'_t \\ \hat{\dot{q}}_{t'+dt} = \hat{\dot{q}}_{t'} + \hat{\ddot{q}}_{t'+dt}dt, \\ \hat{q}_{t'+dt} = \hat{q}_{t'} + \hat{\dot{q}}_{t'+dt}dt. \end{cases}$$

Once the trajectory $\hat{q}(t', \dot{q}, q_v)$ has been simulated over a sufficiently long horizon T, it is possible to obtain the distances to the position and velocity constraints as

$$\begin{aligned} \Delta^{pos} &= \min_{t'\in[t,t+T]}\left\{\min_{i\in\{1,\dots,n\}}\left\{\hat{q}_{t',i} - q_{min,i}, q_{max,i} - \hat{q}_{t',i}\right\}\right\}, \\ \Delta^{vel} &= \min_{t'\in[t,t+T]}\left\{\min_{i\in\{1,\dots,n\}}\left\{\hat{\dot{q}}_{t',i} - \dot{q}_{min,i}, \dot{q}_{max,i} - \hat{\dot{q}}_{t',i}\right\}\right\}, \\ \Delta^{\tau} &= \min_{t'\in[t,t+T]}\left\{\min_{i\in\{1,\dots,n\}}\left\{\hat{\tau}_{t',i} - \tau_{min,i}, \tau_{max,i} - \hat{\tau}_{t',i}\right\}\right\}. \end{aligned} \tag{21}$$

respectively.

The overall trajectory-based DSM, Δ_T, can be computed as

$$\Delta_T(q, \dot{q}, q_v) = \min\left\{k^{pos}\Delta^{pos}, k^{vel}\Delta^{vel}, k^{\tau}\Delta^{\tau}\right\}, \tag{22}$$

with positive real gains k^{pos}, k^{vel}, k^{τ}. These design parameters can be used to scale arbitrarily the impact of the distances in the final computation of the DSM.

To ensure that constraints are never violated, in line of principle, the predict horizon should be extended to infinite. To do this, it is sufficient to ensure that, from $t+T$ onward, the closed-loop system dynamics will not exceed a terminal energy constraint. Therefore, we can considered for the system (4), the following energy function [7]:

$$\begin{aligned} V(t) &= \frac{1}{2}\dot{q}^T B(q)\dot{q} \\ &+ mg(q_{qp4} - q_{qp4}C_{q_{p2}}C_{q_{p3}} + l_p - l_p C_{q_{p5}}C_{q_{p6}}) \\ &+ \frac{1}{2}\tilde{q}_r^T K_{pr}\tilde{q}_r + \frac{1}{2}K_{Pl}\tilde{q_l}^2 + \frac{1}{2}K_{Px}\tilde{q_x}^2. \end{aligned} \tag{23}$$

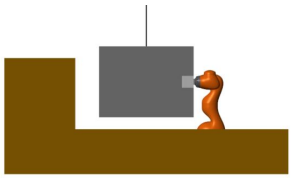

Figure 5. Simulation scenario.

Then, we can compute the terminal energy of the system evaluating (23) at the end of the predicted trajectory, and we can add this cost in the evaluation of the overall Dynamic Safety margin considering

$$\Delta_V(q, \dot{q}, q_v) = k^{E_{term}}(E_{term} - V(\hat{q}_{t'}, \hat{\dot{q}}_{t'}, q_v)), \tag{24}$$

where $k^{E_{term}}$ is a positive real arbitrary scaling factor and $E_{term} > 0$ is a suitable threshold value.

Gathering all of the above, the overall DSM for an infinite time horizon is,

$$\Delta(q, \dot{q}, q_v) = \max\left\{\min(\Delta_T, \Delta_V), 0\right\}. \tag{25}$$

As can be seen in (25), in case the next applied reference violates the system constraints, the DSM will be equal to 0. This means that the internal control loop will be fed with the previous applied reference which guarantees satisfaction constraints.

4 Simulation Results

The aim of this section is to show that: *i*) the proposed control scheme is able to perform correct and safe manipulation of a heavy suspended element; *ii*) the proposed controller works better than the preliminary control scheme proposed in [7].

The simulation scenario we considered is the following: the robotic arm has to move the suspended object with a weight of **100kg**, along the x-axis of $0.2cm$ and along the z-axis of $0.1cm$, in order to place the object in its final position. The robotic arm used in the simulations, a KUKA IIWA14 R820, can handle a payload of up to **14kg**, [16]. However, due to the fact that the mass of the block is sustained almost entirely by the cable, we can still use a lightweight robotic arm to perform the foreseen operations. In this case, the robot assumes the role of precision unit during the positioning of the suspended element.

In the following treatment, the angles will be expressed in degrees while the lengths in centimeters.

We set the initial condition of the system to

$$\begin{aligned} q_r(0) &= [0, 0, 0, -90, -90, 90, 0]^T \\ q_p(0) &= [0, 0, 0, 0.1, 0, 0, 0]^T. \end{aligned}$$

For the desired configurations, we set a first desired reference for the x displacement as

$$r_1 = [-14.4, 6.6, -13.7, -83.2, -88.2, 62, -0.45, 0.2, 0.1]^T$$

and after 25 second, the reference is set so that the object is lowered

$$r_2 = [-13.9, 8.3, -14.2, -95.8, -95.3, 62.3, 15.6, 0.2, 0.2]^T$$

imitating the approach and the placement of a block.

Moreover, the values of the actuator saturation (8), operating region (6), and speed limitation (7) are set as (see [16] for more details regarding the robotic arm used in this work),

$$\begin{aligned}
-\tau_{min,r} &= \tau_{max,r} = [320, 320, 170, 170, 110, 40, 40]^T \text{ Nm},\\
-\tau_{min,x,l} &= \tau_{max,x,l} = 2 \times 10^3 \text{Nm},\\
-q_{min,r} &= q_{max,r} = [170, 120, 170, 120, 170, 120, 175]^T \text{ deg},\\
-q_{min,l} &= 0\text{m}, q_{max,l} = 4\text{m}, \quad -q_{min,x} = q_{max,x} = -2\text{m},\\
-\dot{q}_{min,r} &= \dot{q}_{max,r} = [85, 85, 100, 75, 130, 135, 135]^T \text{ deg/s}\\
-\dot{q}_{min,l} &= \dot{q}_{max,l} = 5\text{m/s}, \quad -\dot{q}_{min,x} = \dot{q}_{max,x} = 3\text{m/s}.
\end{aligned}$$

The PD control gains in (9)-(10) were chosen as

$$\begin{aligned}
K_{Pr} &= \text{diag}([300, 300, 300, 300, 300, 300, 300]),\\
K_{Dr} &= \text{diag}([10, 10, 10, 10, 10, 10, 10]),\\
K_{Px} &= K_{Pl} = 1 \times 10^3,\\
K_{Dx} &= K_{Dl} = 5 \times 10^2,
\end{aligned}$$

The smoothing parameter of the attraction field (14) is $\eta = 1e^{-4}$. This value has been chosen in order to eliminate numerical noise in the attraction field that can occur when q_v is very close to r. The parameters of the repulsion field (17)-(19) are $\zeta = 0.3$, and $\delta = 0.01$. The parameters of the Dynamic Safety Margin defined in (22) are chosen as $k^{pos} = 0.8$, $k^{vel} = 0.5$, $k^{\tau} = 0.01$, $k^{E_{term}} = 15$. These gains are chosen such that the various DSMs of the active constraints have the same order of magnitude. The prediction sampling time to simulate the dynamic of the system is fixed to 1 ms, and with 100 prediction samples we predict over a time horizon of 100 ms. The terminal energy constraint is set to $E_{term} = 150J$. It is important to remember that since the weight of the block is supported by the cable, the internal control of the robot has been developed to ensure high precision in positioning and to avoid elastic deformations of the links of the lightweight robotic arms used in the following simulations.

As one can see in Fig.6-7 the ERG modified the commanded reference r in order to avoid that the constraints are violated and the inner controller is able to move the system robot+object through the applied reference. In particular, as one can seen in Fig.10, the commanded reference is modified in such a way that the speed constraints are never violated. Moreover, the non-actuated variables for the suspended object are damped by the robot during the movement (see Fig.8). It is important to notice that, despite the limitations of payload that can be managed by the robot, the ERG modifying the applied reference taking into account the constraints, it ensures that the robot is never overloaded. In fact, as one can see in Fig.9, the torque required to the robotic actuators are well within the joint torques limits. Finally, we show why a governing unit is necessary by analyzing the behaviour of the control scheme proposed in [7] considering the same simulation scenario discussed so far. In Fig.11 is shown the time evolution for the joint robot torque related to the control scheme proposed in [7]. This control scheme is based on a trajectory pre-evaluated off line and for this reason, it does not take into account any constraints (and in particular the torques robot saturation). Therefore, if no off-line trajectory is calculated, when there are sudden changes in the reference (*i.e.* at the beginning and at about 25 seconds), the torques required by the robot actuators violate the maximum (or the minimum) limits. This leads to an overload of the robot and makes the operation unfeasible.

5 Conclusions

This paper proposed a constrained control scheme based on the ERG framework for the control of a mechanical system to place heavy prefabricated elements. Based on the previous results already present in the scientific community, the aim of this paper is to propose a control scheme that is able to overcome the limitations of the works proposed so far by enforcing an inner loop controller with an external control unit that is able to manage the constraints of the system. In the first part of this paper a mathematical model of the overall system is derived, and then the constrained control scheme is described. Simulation results show that the proposed control scheme is able to fulfill the constraints of the system while moving the suspended object to its final position. It is worth noting that no off-line trajectory has been calculated that it is the control law itself that decides how to move the reference to avoid constraints violations. Moreover, future research will focus on the possibility of mounting the robot on a mobile base in order to guarantee easy movement in the working environment.

6 Acknowledgments

This research has been funded by The Brussels Institute for Research and Innovation (INNOVIRIS) of the Brussels Region through the Applied PHD grant: Brickiebots -

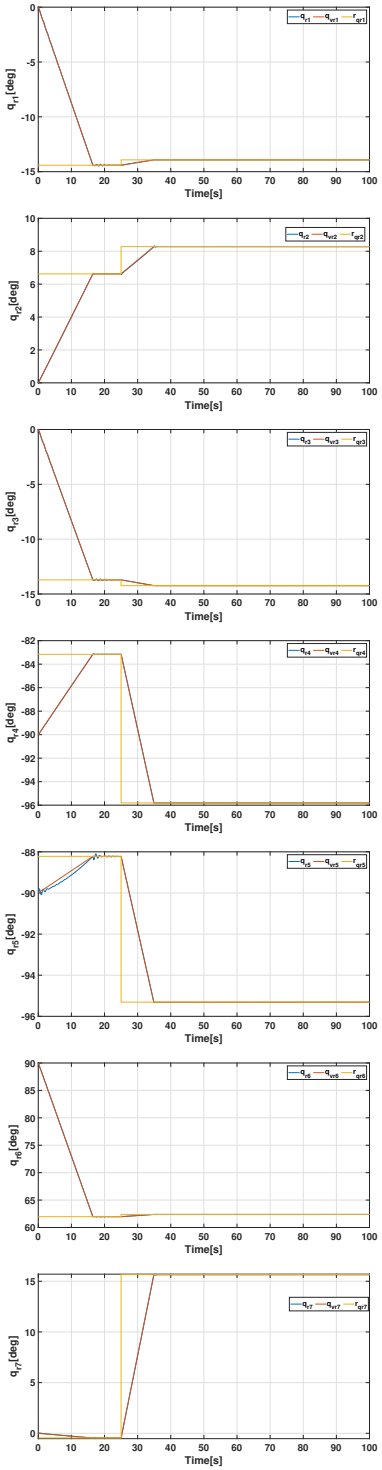

Figure 6. Time evolution of joint robot positions.

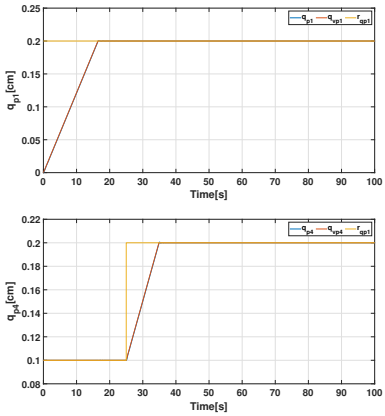

Figure 7. Time evolution of actuated joints of the suspended element positions.

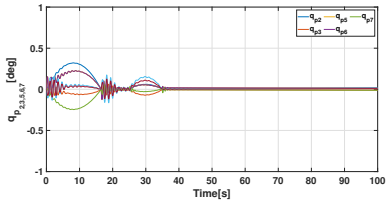

Figure 8. Time evolution of non-actuated joints of the suspended element positions.

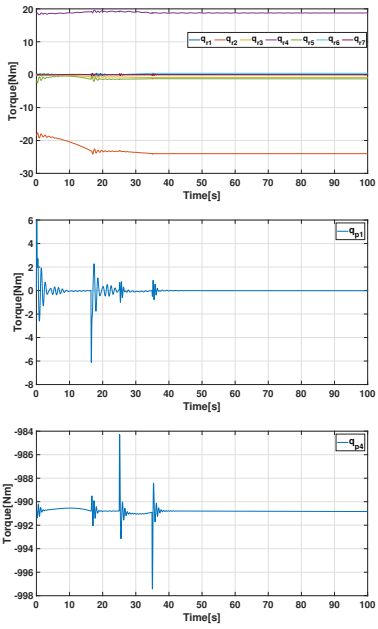

Figure 9. Time evolution of the requires torques.

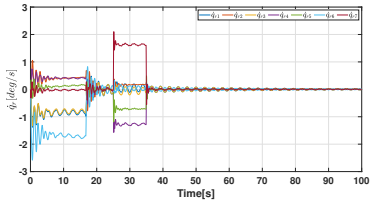

Figure 10. Time evolution of joint robot speed.

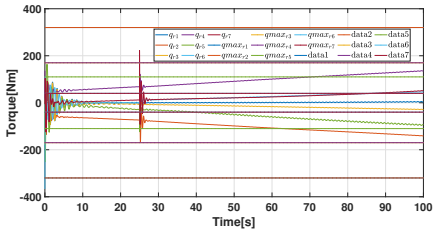

Figure 11. Time evolution of joint robot torques for the control scheme [7].

Robotic Bricklayer: a multi-robot system for sand-lime blocks masonry (réf : 19-PHD-12).

References

[1] Sung-Min Moon, Jaemyung Huh, Daehie Hong, Seunghoon Lee, and Chang-Soo Han. Vertical motion control of building facade maintenance robot with built-in guide rail. *Robotics and Computer-Integrated Manufacturing*, 31:11–20, 2015.

[2] Marwan Gharbia, Alice Chang-Richards, Yuqian Lu, Ray Y Zhong, and Heng Li. Robotic technologies for on-site building construction: A systematic review. *Journal of Building Engineering*, 32:101584, 2020.

[3] Constructon site accidents. `https://www.attorneystevelee.com/our-library/types-of-construction-site-accidents/`.

[4] J. Andres, Thomas Bock, F. Gebhart, and W. Steck. First results of the development of the masonry robot system rocco. *Proceedings of the 11th ISARC*, pages 87–93, 01 1994.

[5] Marwan Gharbia, Alice Chang-Richards, Yuqian Lu, Ray Y Zhong, and Heng Li. Robotic technologies for on-site building construction: A systematic review. *Journal of Building Engineering*, page 101584, 2020.

[6] Michele Ambrosino, Philippe Delens, and Emanuele Garone. Control of a multirobot bricklaying system. *Advanced Control for Applications: Engineering and Industrial Systems*, 3(4):e90, 2021.

[7] Michele Ambrosino, Philippe Delens, and Emanuele Garone. Modeling and control of multi-units robotic system: Boom crane and robotic arm. In *Proceedings of the 38th International Symposium on Automation and Robotics in Construction (ISARC)*, pages 789–796. International Association for Automation and Robotics in Construction (IAARC), November 2021. doi:10.22260/ISARC2021/0107.

[8] S Joe Qin and Thomas A Badgwell. An overview of nonlinear model predictive control applications. *Nonlinear model predictive control*, pages 369–392, 2000.

[9] Michael Nikolaou. Model predictive controllers: A critical synthesis of theory and industrial needs. 2001.

[10] Emanuele Garone, Stefano Di Cairano, and Ilya Kolmanovsky. Reference and command governors for systems with constraints: A survey on theory and applications. *Automatica*, 75:306–328, 2017.

[11] Marco M. Nicotra and Emanuele Garone. The explicit reference governor: A general framework for the closed-form control of constrained nonlinear systems. *IEEE Control Systems Magazine*, 38(4):89–107, 2018. doi:10.1109/MCS.2018.2830081.

[12] Michele Ambrosino, Arnaud Dawans, and Emanuele Garone. Constraint control of a boom crane system. In *Proceedings of the 37th International Symposium on Automation and Robotics in Construction (ISARC)*. International Association for Automation and Robotics in Construction (IAARC), October 2020. ISBN 978-952-94-3634-7. doi:10.22260/ISARC2020/0069.

[13] Günter Schreiber, Andreas Stemmer, and Rainer Bischoff. The fast research interface for the kuka lightweight robot. In *IEEE workshop on innovative robot control architectures for demanding (Research) applications how to modify and enhance commercial controllers (ICRA 2010)*, pages 15–21. Citeseer, 2010.

[14] Gustavo M Freitas, Antonio C Leite, and Fernando Lizarralde. Kinematic control of constrained robotic systems. *Sba: Controle & Automação Sociedade Brasileira de Automatica*, 22:559–572, 2011.

[15] Elie Hermand, Tam W Nguyen, Mehdi Hosseinzadeh, and Emanuele Garone. Constrained control of uavs in geofencing applications. In *2018 26th Mediterranean Conference on Control and Automation (MED)*, pages 217–222. IEEE, 2018.

[16] Kuka. `https://www.kuka.com/`.